

This Page Is Inserted by IFW Operations
and is not a part of the Official Record

BEST AVAILABLE IMAGES

Defective images within this document are accurate representations of the original documents submitted by the applicant.

Defects in the images may include (but are not limited to):

- BLACK BORDERS
- TEXT CUT OFF AT TOP, BOTTOM OR SIDES
- FADED TEXT
- ILLEGIBLE TEXT
- SKEWED/SLANTED IMAGES
- COLORED PHOTOS
- BLACK OR VERY BLACK AND WHITE DARK PHOTOS
- GRAY SCALE DOCUMENTS

IMAGES ARE BEST AVAILABLE COPY.

**As rescanning documents *will not* correct images,
please do not report the images to the
Image Problem Mailbox.**

The Journal of Clinical Investigation

January 1, 1996, Volume 97, Number 1

Editorials

- The times they are still a'changing: keeping up with the times.
A.P. Varki 1
- Molecular Medicine in genetically engineered animals: series introduction.
K.R. Chien 2

Perspectives

- Gene modification via "plug and socket" gene targeting. J. Lewis, B. Yang,
P. Dettliff, and O. Smithies 3

Regular Articles

- Digoxin reduces β -adrenergic contractile response in rabbit hearts.
 Ca^{2+} -dependent inhibition of adenylyl cyclase activity via Na^+/Ca^{2+}
exchange. K. Nagai, T. Murakami, T. Iwase, T. Tomita, and S. Sasayama 6
- Sex steroids, bone mass, and bone loss. A prospective study of pre-,
peri-, and postmenopausal women. C. Slemenda, C. Longcope,
M. Peacock, S. Hui, and C.C. Johnston 14
- Vitamin C improves endothelium-dependent vasodilation in patients
with non-insulin-dependent diabetes mellitus. H.H. Ting, F.K. Timimi,
K.S. Boles, S.J. Creager, P. Ganz, and M.A. Creager 22
- Red cell membrane remodeling in sickle cell anemia. Sequestration of
membrane lipids and proteins in heinz bodies. S.-C. Liu, S.J. Yi,
J.R. Mehta, P.E. Nichols, S.K. Ballas, P.W. Yacono, D.E. Golan,
and J. Palek 29
- Distribution and regulation of plasminogen activator inhibitor-1 in
murine adipose tissue in vivo. Induction by tumor necrosis factor- α
and lipopolysaccharide. F. Samad, K. Yamamoto, and D.J. Loskutoff 37
- Functional magnetic resonance imaging reveals brain regions mediating
the response to resistive expiratory loads in humans. D. Gozal,
O. Omidvar, K.A.T. Kirlew, G.M. Hathout, R.B. Lufkin,
and R.M. Harper 47
- Modulation of L-Selectin ligand expression during an immune response
accompanying tumorigenesis in transgenic mice. S.V. Onrust,
P.M. Hartl, S.D. Rosen, and D. Hanahan 54
- Prolonged postprandial responses of lipids and apolipoproteins in
triglyceride-rich lipoproteins of individuals expressing an apolipoprotein
e4 allele. N. Bergeron and R.J. Havel 65
- Accumulation of methotrexate polyglutamates in lymphoblasts is a
determinant of antileukemic effects in vivo. A rationale for high-dose
methotrexate. E. Masson, M.V. Relling, T.W. Synold, Q. Liu,
J.D. Schuetz, J.T. Sandlund, C.H. Pui, and W.E. Evans 73
- Comparison of the time courses of insulin and the portal signal on
hepatic glucose and glycogen metabolism in the conscious dog.
M.J. Pagliassotti, L.C. Holste, M.C. Moore, D.W. Neal,
and A.D. Cherrington 81
- Gastric emptying and release of incretin hormones after glucose
ingestion in humans. J. Schirra, M. Katschinski, C. Weidmann,
T. Schäfer, U. Wank, R. Arnold, and B. Göke 92
- Increased δ aminolevulinic acid and decreased pineal melatonin
production. H. Puy, J.-C. Deybach, A. Bogdan, J. Callebort,
J. Baumgartner, P. Voisin, Y. Nordmann, and Y. Touitou 104
- Anti-endothelial cell autoantibodies from scleroderma patients
induce leukocyte adhesion to human vascular endothelial cells in vitro.
D. Carullo, C.O.S. Savage, C.M. Black, and J.D. Pearson 111
- Role of angiotensin II in dietary modulation of rat late distal tubule
bicarbonate flux in vivo. D.Z. Levine, M. Iacovitti, S. Buckman,
and K.D. Burns 120
- Direct assessment of liver glycogen storage by ^{13}C nuclear magnetic
resonance spectroscopy and regulation of glucose homeostasis after
mixed meal in normal subjects. R. Taylor, I. Magnusson,
J. Rothman, G.W. Cline, A. Caumo, C. Cobelli, and G.I. Shulman 126
- Elimination of the action of glucagon-like peptide 1 causes an
impairment of glucose tolerance after nutrient ingestion by healthy
baboons. D.A. D'Alessio, R. Vogel, R. Prigeon, E. Luszczansky,
D. Koerker, J. Eng, and J.W. Ensinck 133
- G-protein coupled and tyrosine kinase receptors: evidence that
activation of the insulin-like growth factor I receptor is required for
thrombin-induced mitogenesis of rat aortic smooth muscle cells.
P. Delafontaine, A. Anwar, H. Lou, and L. Ku 139
- Induction of cyclin A gene expression by homocysteine in vascular
smooth muscle cells. J.-C. Tsai, H. Wang, M.A. Perrella,
M. Yoshizumi, N.E.S. Sibinga, L.C. Tian, E. Haber,
T.H.-T. Chang, R. Schlegel, and M.-E. Lee 146
- Profound induction of hepatic cholesteryl ester transfer protein
transgene expression in apolipoprotein E and low density
lipoprotein receptor gene knockout mice. L. Masucci-Magoulas,
A. Plump, X.C. Jiang, A. Walsh, J.L. Breslow, and A.R. Tall 154
- Involvement of wound-associated factors in rat brain astrocyte
migratory response to axonal injury: in vitro simulation. A. Faber-Elman,
A. Solomon, J.A. Abraham, M. Marikovsky, and M. Schwartz 162
- Inhibition of cyclic 3'-5'-guanosine monophosphate-specific
phosphodiesterase selectively vasodilates the pulmonary circulation
in chronically hypoxic rats. A.H. Cohen, K. Hanson, K. Morris,
B. Fouty, L.F. McMurtry, W. Clarke, and D.M. Rodman 172
- Mechanism of impaired glucose-potentiated insulin secretion in
diabetic 90% pancreatectomy rats. Study using glucagon-like peptide-1
(7-37). Y.A. Hosokawa, H. Hosokawa, C. Chen, and J.L. Leahy 180
- Heparin-binding secretory transforming gene (*hst*) facilitates rat
lactotrope cell tumorigenesis and induces prolactin gene transcription.
I. Shimon, A. Hüttner, J. Said, O.M. Spirina, and S. Melmed 187
- A single strand conformation polymorphism study of cd40 ligand.
Q. Lin, J. Rohrer, R.C. Allen, M. Larché, J.M. Greene, A.O. Shigeoka,
R.A. Gatti, D.C. Derauf, J.W. Belmont, and M.E. Conley 196
- Maternal vasoactive intestinal peptide and the regulation of embryonic
growth in the rodent. J.M. Hill, S.K. McCune, R.J. Alvero, G.W. Glazner,
K.A. Henins, S.F. Stanziale, J.R. Keimowitz, and D.E. Brememan 202
- Cerebral protection in homozygous null ICAM-1 mice after middle
cerebral artery occlusion. Role of neutrophil adhesion in the
pathogenesis of stroke. E.S. Connolly, Jr., C.J. Winfree,
T.A. Springer, Y. Naka, H. Liao, S.D. Yan, D.M. Stern,
R.A. Solomon, J.-C. Gutierrez-Ramos, and D.J. Pinsky 209
- Allogeneic hematolymphoid microchimerism and prevention of
autoimmune disease in the rat. A relationship between allo- and
autoimmunity. C.P. Delaney, N. Murase, M. Chen-Woan, J.J. Fung,
T.E. Starzl, and A.J. Demetris 217

Rapid Publications

- Transient introduction of a foreign gene into healing rat patellar
ligament. N. Nakamura, S. Horibe, N. Matsumoto, T. Tomita,
T. Natsuume, Y. Kaneda, K. Shino, and T. Ochi 226
- Bleomycin-induced pulmonary fibrosis in transgenic mice that either
lack or overexpress the murine plasminogen activator inhibitor-1
gene. D.T. Eitzman, R.D. McCoy, X. Zheng, W.P. Fay,
T. Shen, D. Ginsburg, and R.H. Simon 232
- Receptor-mediated endothelial cell dysfunction in diabetic
vasculopathy. Soluble receptor for advanced glycation end
products blocks hyperpermeability in diabetic rats. J.-L. Wautier,
C. Zoukourian, O. Chappey, M.-P. Wautier, P.-J. Guillausseau,
R. Cao, O. Hori, D. Stern, and A.M. Schmidt 238
- Interleukin 6 receptor antibody inhibits muscle atrophy and modulates
proteolytic systems in interleukin 6 transgenic mice. T. Tsujinaka,
J. Fujita, C. Ebisui, M. Yano, E. Kominami, K. Suzuki, K. Tanaka,
A. Katsume, Y. Ohsugi, H. Shiozaki, and M. Monden 244

Applicants: David J. Pinsky
U.S. Serial No.: 09/374,586
Filed: August 13, 1999
Group Art Unit: 1633

Cerebral Protection in Homozygous Null ICAM-1 Mice after Middle Cerebral Artery Occlusion

Role of Neutrophil Adhesion in the Pathogenesis of Stroke

E. Sander Connolly, Jr.,* Christopher J. Winfree,* Timothy A. Springer,^{||} Y. Shifumi Naka,[†] Hui Liao,[‡] Shi Du Yan,[‡] David M. Stern,[‡] Robert A. Solomon,* Jose-Carlos Gutierrez-Ramos,^{||} and David J. Pinsky[§]

Departments of *Neurosurgery, [†]Physiology, and [‡]Medicine, Columbia University, College of Physicians and Surgeons, New York 10032; and ^{||}The Center for Blood Research, Harvard Medical School, Boston, Massachusetts 02138

Abstract

Acute neutrophil (PMN) recruitment to postischemic cardiac or pulmonary tissue has deleterious effects in the early reperfusion period, but the mechanisms and effects of neutrophil influx in the pathogenesis of evolving stroke remain controversial. To investigate whether PMNs contribute to adverse neurologic sequelae and mortality after stroke, and to study the potential role of the leukocyte adhesion molecule intercellular adhesion molecule-1 (ICAM-1) in the pathogenesis of stroke, we used a murine model of transient focal cerebral ischemia consisting of intraluminal middle cerebral artery occlusion for 45 min followed by 22 h of reperfusion. PMN accumulation, monitored by deposition of ¹¹¹In-labeled PMNs in postischemic cerebral tissue, was increased 2.5-fold in the ipsilateral (infarcted) hemisphere compared with the contralateral (noninfarcted) hemisphere ($P < 0.01$). Mice immunodepleted of neutrophils before surgery demonstrated a 3.0-fold reduction in infarct volumes ($P < 0.001$), based on triphenyltetrazolium chloride staining of serial cerebral sections, improved ipsilateral cortical cerebral blood flow (measured by laser Doppler), and reduced neurological deficit compared with controls. In wild-type mice subjected to 45 min of ischemia followed by 22 h of reperfusion, ICAM-1 mRNA was increased in the ipsilateral hemisphere, with immunohistochemistry localizing increased ICAM-1 expression on cerebral microvascular endothelium. The role of ICAM-1 expression in stroke was investigated in homozygous null ICAM-1 mice (ICAM-1 $-/-$) in comparison with wild-type controls (ICAM-1 $+/+$). ICAM-1 $-/-$ mice demonstrated a 3.7-fold reduction in infarct volume ($P < 0.005$), a 35% increase in survival ($P < 0.05$), and reduced neurologic deficit compared with ICAM-1 $+/+$ controls. Cerebral blood flow to the infarcted hemisphere was 3.1-fold greater in ICAM-1 $-/-$ mice compared with ICAM-1 $+/+$ controls ($P < 0.01$), suggesting an important role for ICAM-1 in the genesis of postischemic cerebral no-reflow. Because PMN-depleted and ICAM-1-deficient mice are relatively resistant to cerebral ischemia-reperfusion injury, these studies suggest an important role for ICAM-1-mediated PMN adhesion in the pathophysiology of evolving stroke. (*J. Clin. Invest.* 1996; 97:209–216)

Address correspondence to David J. Pinsky, M.D., Columbia University, P & S 11-518, 630 W. 168th St., New York, NY 10032. Phone: 212-305-1615; FAX: 212-305-5337.

Received for publication 12 June 1995 and accepted in revised form 19 September 1995.

J. Clin. Invest.

© The American Society for Clinical Investigation, Inc.

0021-9738/96/01/0209/08 \$2.00

Volume 97, Number 1, January 1996, 209–216

Key words: cerebral ischemia • stroke • neutrophil • ICAM-1

Introduction

Neutrophils (PMNs) are critically involved in the earliest stages of inflammation after tissue ischemia, initiating scavenger functions which are later subsumed by macrophages. However, there is a darker side to neutrophil influx, especially in postischemic tissues (1–7), where activated PMNs may augment damage to vascular and parenchymal cellular elements. Experimental evidence points to a pivotal role for endothelial cells in establishing postischemic PMN recruitment, in that hypoxic/ischemic endothelial cells synthesize the proinflammatory cytokine IL-1 (8) as well as the potent neutrophil chemoattractant and activator IL-8 (9). Firm adhesion of PMNs to activated endothelium in a postischemic vascular milieu is promoted by translocation of P-selectin to the cell surface (10) as well as enhanced production of platelet activating factor (PAF) and intercellular adhesion molecule-1 (ICAM-1) (11).

While strategies to block each of these mechanisms of neutrophil recruitment are protective in various models of ischemia and reperfusion injury, their effectiveness in cerebral ischemia/reperfusion injury remains controversial. There is considerable evidence that in the brain, as in other tissues, an early PMN influx follows an ischemic episode (12–17). Immunohistochemical studies have described increased expression of the PMN adhesion molecules P-selectin and ICAM-1 in the postischemic cerebral vasculature (12, 18–20). The pathogenic relevance of adhesion molecule expression in the brain remains controversial, however; data from a trial of a monoclonal anti-ICAM-1 antibody in stroke in humans are not yet available (Rothlein, R., personal communication). In animal models, there is conflicting experimental evidence regarding the effectiveness of anti-adhesion molecule strategies in the treatment of experimental stroke (21–23). To determine whether ICAM-1 participates in the pathogenesis of postischemic cerebral injury, the experiments reported here were undertaken in a murine model of focal cerebral ischemia and reperfusion so that the role of a single, critical mediator of PMN adhesion (ICAM-1) could be determined. These studies demonstrate that enhanced ICAM-1 expression and neutrophil influx follow an episode of focal cerebral ischemia. Furthermore, these studies show that both neutrophil-deficient and transgenic ICAM-1 null mice are relatively resistant to cerebral infarction after ischemia and reperfusion, providing strong evidence for an exacerbating role of ICAM-1 in the pathophysiology of stroke.

1. Abbreviations used in this paper: ICAM-1, intercellular adhesion molecule-1; PAF, platelet activating factor; TTC, 2,3,5, triphenyl, 2H-tetrazolium chloride.

Methods

Mice. Experiments were performed with transgenic ICAM-1-deficient mice created as reported previously (24) by gene targeting in J1 embryonic stem cells, injected into C57BL/6 blastocysts to obtain germline transmission and backcrossed to obtain homozygous null ICAM-1 mice. All experiments were performed with ICAM-1 $-/-$ or wild-type (ICAM-1 $+/-$) cousin mice from the fifth generation of backcrossings with C57BL/6 mice. Animals were 7–9 wk of age and weighed between 25 and 36 grams at the time of experiments. For certain experiments, neutrophil depletion of C57BL/6 mice was accomplished by administering polyclonal rabbit anti-mouse neutrophil antibody (25) (Accurate Chemical & Scientific Corp., Westbury, NY) preadsorbed to red blood cells as a daily intraperitoneal injection (0.3 ml of 1:12 solution) for 3 d. Experiments in these mice were performed on the fourth day after confirming agranulocytosis by Wright-Giemsa-stained peripheral blood smears.

Transient middle cerebral artery occlusion (26). Mice were anesthetized with an intraperitoneal injection of 0.3 ml of ketamine (10 mg/ml) and xylazine (0.5 mg/ml). Animals were positioned supine on a rectal temperature-controlled operating surface (Yellow Springs Instrument Co., Yellow Springs, OH). Animal core temperature was maintained at 36–38°C intraoperatively and for 90 min postoperatively. Middle cerebral artery occlusion was performed as follows: A midline neck incision was created to expose the right carotid sheath under the operating microscope (16–25 \times zoom; Carl Zeiss, Inc., Thornwood, NY). The common carotid artery was freed from its sheath and isolated with a 4-0 silk, and the occipital and pterygopalatine arteries were each isolated and divided. Distal control of the internal carotid artery was obtained, and the external carotid was cauterized and divided just proximal to its bifurcation into the lingual and maxillary divisions. Transient carotid occlusion was accomplished by advancing a 13-mm heat-blunted 5-0 nylon suture via the external carotid stump to the origin of the middle cerebral artery. After placement of the occluding suture, the external carotid artery stump was cauterized to prevent bleeding through the arteriotomy, and arterial flow was reestablished. In all cases, the duration of carotid occlusion was < 2 min. After 45 min, the occluding suture was withdrawn to establish reperfusion. These procedures have been described previously in detail (26).

Measurement of cerebral cortical blood flow. Transcranial measurements of cerebral blood flow were made using laser Doppler flow measurements (Perimed, Inc., Piscataway, NJ) after reflection of the skin overlying the calvarium, as described previously (27) (transcranial readings were consistently the same as those made after craniectomy in pilot studies). Using a 0.7-mm straight laser Doppler probe (model PF303; Perimed, Inc.) and previously published landmarks (2 mm posterior to the bregma, 6 mm to each side of midline), relative cerebral blood flow measurements were made as indicated: immediately after anesthesia, after occlusion of the middle cerebral artery, immediately after reperfusion, and at 24 h just before euthanasia. Data are expressed as the ratio of the Doppler signal intensity of the ischemic compared with the nonischemic hemisphere. Although this method does not quantify cerebral blood flow per gram of tissue, use of laser Doppler flow measurements at precisely defined anatomic landmarks serves as a means of comparing cerebral blood flows in the same animal serially over time. The surgical procedure/intraluminal middle cerebral artery occlusion and reperfusion were considered to be technically adequate if $\geq 50\%$ reduction in relative cerebral blood flow was observed immediately after placement of the intraluminal occluding suture and a $\geq 33\%$ increase in flow over baseline occlusion was observed immediately after removal of the occluding suture. These methods have been used in previous studies (26).

Preparation and administration of ^{111}In -labeled murine neutrophils. Citrated blood from wild-type mice was diluted 1:1 with NaCl (0.9%) followed by gradient ultracentrifugation on Ficoll-Hypaque (Pharmacia LKB Biotechnology, Inc., Piscataway, NJ). After hypotonic lysis of residual erythrocytes (20-s exposure to distilled H_2O fol-

lowed by reconstitution with 1.8% NaCl), the neutrophils were suspended in PBS. $5\text{--}7.5 \times 10^6$ neutrophils were suspended in PBS with 100 μCi of ^{111}In oxine (Amersham Mediphsysics, Port Washington, NY) for 15 min at 37°C. After washing with PBS, the neutrophils were gently pelleted (450 g) and resuspended in PBS to a final concentration of 1.0×10^6 cells/ml. Immediately before surgery, 100 μl of radiolabeled PMNs admixed with physiologic saline to a total volume of 0.3 ml ($\approx 3 \times 10^6$ cpm) was administered by penile vein injection. After humane killing, brains were obtained as described, and neutrophil deposition quantified as counts per minute per gram of each hemisphere.

Neurological exam. 24 h after middle cerebral artery occlusion and reperfusion, before giving anesthesia, mice were examined for neurological deficit using a four-tiered grading system (26). A score of 1 was given if the animal demonstrated normal spontaneous movements; a score of 2 was given if the animal was noted to be turning to the right (clockwise circles) when viewed from above (i.e., toward the contralateral side); a score of 3 was given if the animal was observed to spin longitudinally (clockwise when viewed from the tail); and a score of 4 was given if the animal was crouched on all fours, unresponsive to noxious stimuli. This scoring system has been described previously in mice (26) and is based upon similar scoring systems used in rats (28, 29) which are based upon the contralateral movement of animals with stroke; after cerebral infarction, the contralateral side is "weak" and so the animal tends to turn toward the weakened side. Previous work in rats (28) and mice (26) demonstrates that larger cerebral infarcts are associated with a greater degree of contralateral movement, up to the point where the infarcts are so large that the animal remains unresponsive.

Calculation of infarct volume. After neurologic examination, mice were given 0.3 ml of ketamine (10 mg/ml) and xylazine (0.5 mg/ml), and final cerebral blood flow measurements were obtained. Humane killing was performed by decapitation under anesthesia, and brains were removed and placed in a mouse brain matrix (Activational Systems, Inc., Warren, MI) for 1-mm sectioning. Sections were immersed in 2% 2,3,5, triphenyl, 2H-tetrazolium chloride (TTC; Sigma Chemical Co., St. Louis, MO) in 0.9% PBS, incubated for 30 min at 37°C, and placed in 10% formalin (26, 30–32). Infarcted brain was visualized as an area of unstained tissue, in contrast to viable tissue, which stains brick red. Infarct volumes were calculated from planimetric serial sections and expressed as the percentage of infarct in the ipsilateral hemisphere.

RNA extraction and Northern blot analysis. 24 h after focal ischemia and reperfusion, brains were obtained and divided into ipsilateral (infarct) and contralateral (noninfarct) hemispheres. To detect ICAM-1 transcripts, total RNA was extracted from each hemisphere using an RNA isolation kit (Stratagene, La Jolla, CA). Equal amounts of RNA (20 $\mu\text{g}/\text{lane}$) were loaded onto a 1.4% agarose gel containing 2.2 M formaldehyde for size fractionation and then transferred overnight to nylon (Nytran) membranes with 10 \times SSC buffer by capillary pressure. A murine ICAM-1 cDNA probe (33) (1.90 kb; American Type Culture Collection, Rockville, MD) was labeled with ^{32}P - α -dCTP by random primer labeling (Prime-A-Gene kit; Promega, Madison, WI), hybridized to blots at 42°C, followed by three washes of 1 \times SSC/0.05% SDS. Blots were developed with X-Omat AR film exposed with light screens at -70°C for 7 d. A β -actin probe (American Type Culture Collection) was used to confirm equal RNA loading.

Immunohistochemistry. Brains were removed at the indicated times after middle cerebral artery occlusion, fixed in 10% formalin, paraffin embedded, and sectioned for immunohistochemistry. Sections were stained with a rat anti-murine ICAM-1 antibody (1:50 dilution; Genzyme Corp., Cambridge, MA), and sites of primary antibody binding were visualized by an alkaline phosphatase-conjugated secondary antibody detected with FastRed (TR/naphthol AS-MX; Sigma Chemical Co.).

Data analysis. Cerebral blood flow, infarct volumes, and neurologic outcome scores were compared using Student's *t* test for un-

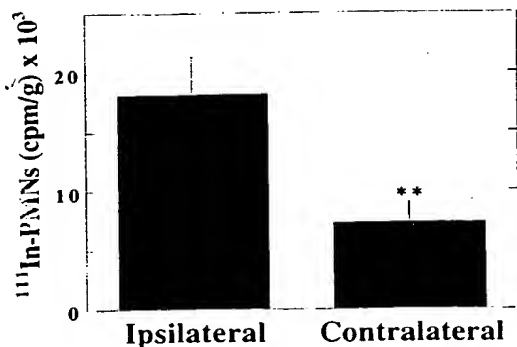


Figure 1. Neutrophil accumulation after focal cerebral ischemia and reperfusion in the mouse. Right middle cerebral artery occlusion was performed for 45 min, followed by 22 h of reperfusion in male C57BL/6 mice. 1 h before middle cerebral artery occlusion, 3.3×10^5 ¹¹¹In-labeled neutrophils were injected into the tail vein. Ipsilateral (right hemispheric) and contralateral (left hemispheric) counts were obtained and normalized per gram of tissue. $n = 7$, ** $P < 0.01$.

paired variables. ¹¹¹In-neutrophil deposition was evaluated as paired data (comparing contralateral [noninfarct] with ipsilateral [infarct] hemisphere), to control for variations in injected counts or volume of distribution. Survival differences between groups were tested using contingency analysis with the χ^2 statistic. Values are expressed as means \pm SEM, with a $P < 0.05$ considered statistically significant.

Results

Neutrophil accumulation in stroke. Previous pathologic studies have shown neutrophil accumulation after cerebral infarc-

tion (15–17, 34–36). To determine whether neutrophils accumulate in our murine model of focal cerebral ischemia and reperfusion, neutrophil accumulation after transient (45 min) ischemia and reperfusion (22 h) was quantified by measuring the deposition of ¹¹¹In-labeled neutrophils given to wild-type mice before the ischemic event. These experiments demonstrated significantly greater neutrophil accumulation (2.5-fold increase) in the ipsilateral (infarcted) compared with the contralateral (noninfarcted) hemispheres ($n = 7$, $P < 0.01$; Fig. 1). Similar results were obtained when neutrophil influx was monitored by myeloperoxidase assays, though low levels of activity were recorded in the latter assay (data not shown).

Effect of neutrophil depletion on stroke outcome. To determine the effect of neutrophil influx on indices of stroke outcome, mice were immunodepleted of neutrophils beginning 3 d before surgery. When surgery was performed on the fourth day, nearly complete agranulocytosis was evident on smears of peripheral blood. Neutropenic mice ($n = 18$) were subjected to 45 min of cerebral ischemia and 22 h of reperfusion, and indices of stroke outcome were determined. Infarct volumes were threefold smaller in neutropenic animals compared with wild-type controls ($11.1 \pm 1.6\%$ vs. $33.1 \pm 6.4\%$, $P < 0.001$; Fig. 2A). The decrease in infarct volumes in neutropenic mice was paralleled by reduced neurologic deficit scores (Fig. 2B), increased postreperfusion cerebral cortical blood flows (Fig. 2C), and a trend toward reduced overnight mortality (22% mortality in neutropenic mice vs. 50% mortality in controls, Fig. 2D).

ICAM-1 expression in murine stroke. To establish the effect of cerebral ischemia/reperfusion in our murine model, ICAM-1 mRNA levels were evaluated after cerebral ischemia and reperfusion in wild-type mice. Ipsilateral (infarcted) cere-

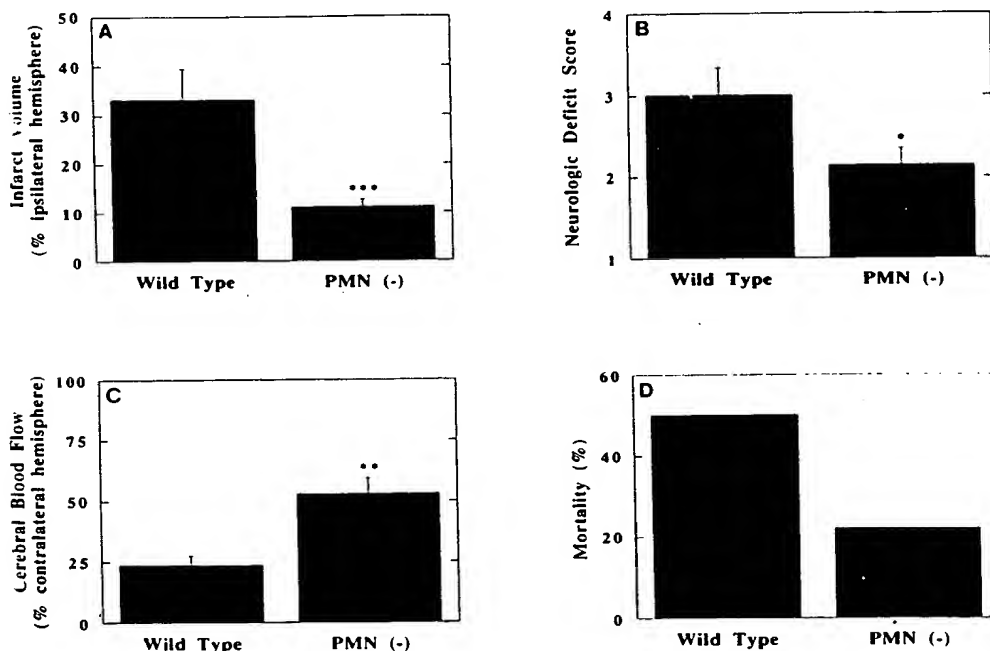
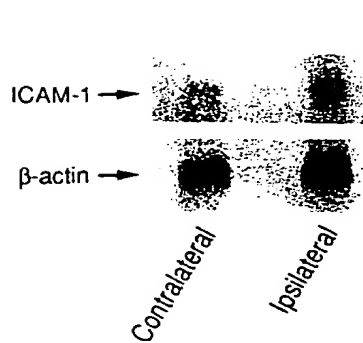


Figure 2. Effect of preoperative neutrophil depletion on indices of stroke outcome. C57BL/6 male mice were subjected to transient middle cerebral artery occlusion as described above (Wild Type, $n = 16$) and compared with a similar procedure performed in mice immunodepleted of neutrophils during the 3 d before the day of surgery (PMN (-), $n = 18$). (A) Infarct volumes were calculated based on TTC-stained serial cerebral sections and were expressed as the percentage of ipsilateral hemispheric volume. (B) Neurologic deficit score was graded before anesthesia 24 h after transient middle cerebral artery occlusion; 4 represents the most severe neurologic deficit. (C) Cerebral blood flow was measured by laser Doppler flow measurements 2 mm posterior to the bregma, expressed as percentage of contralateral hemispheric blood flow. (D) Mortality at 24 h after transient middle cerebral artery occlusion. * $P < 0.05$, ** $P < 0.01$, *** $P < 0.001$.



brane. the Northern blot was probed with a ^{32}P -labeled 1.90-kb murine ICAM-1 cDNA (33) (*top*). A β -actin probe was used for a control (*bottom*).

Figure 3. Expression of ICAM-1 transcripts 24 h after middle cerebral artery occlusion. RNA was prepared from the ipsilateral (infarct) and the contralateral (noninfarct) hemispheres from the same mouse, and an agarose gel was loaded with 20 μg of total RNA per lane. After overnight transfer to a nylon mem-

bral hemisphere demonstrated increased ICAM-1 mRNA by Northern blot analysis compared with RNA obtained from the contralateral (noninfarcted) hemisphere from the same animal (Fig. 3). To evaluate ICAM-1 antigen expression in this murine model, wild-type mice were subjected to 45 min of ischemia followed by 22 h of reperfusion, and the cerebral microvasculature was examined by immunohistochemistry. ICAM-1 antigen expression was not detectable in the cerebral microvasculature contralateral to the infarct (Fig. 4 A), but was markedly increased on the ipsilateral side, with prominent ICAM-1 staining of cerebral endothelial cells (Fig. 4 B).

Role of ICAM-1 in stroke. To explore the role of ICAM-1 in stroke, transgenic mice which were homozygous ICAM-1 deficient (24) were studied in the murine model of focal cerebral ischemia and reperfusion. Because variations in cere-

brovascular anatomy been reported to result in differences in susceptibility to experimental stroke in mice (37), india ink staining was performed on the circle of Willis in homozygous null (ICAM-1 $-/-$) and ICAM-1 $+/+$ mice. These experiments (Fig. 5) demonstrated that there were no gross anatomic differences in the vascular pattern of the cerebral circulation. To determine the role of ICAM-1 in neutrophil influx after focal cerebral ischemia and reperfusion, neutrophil accumulation was measured in homozygous null ICAM-1 mice (ICAM-1 $-/-$) mice ($n = 14$) and wild-type controls ($n = 7$) infused with ^{111}In -labeled neutrophils. Relative neutrophil accumulation (ipsilateral counts per minute/contralateral counts per minute) was diminished (39% reduction) in the ICAM-1 $-/-$ mice compared with ICAM-1 $+/+$ controls (1.70 ± 0.26 vs. 2.9 ± 0.52 , $P < 0.05$).

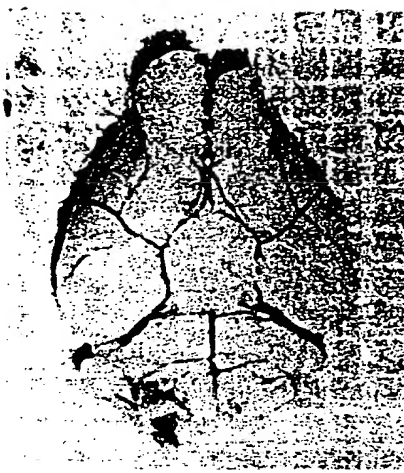
Experiments were then performed to investigate whether expression of ICAM-1 has a pathophysiologic role in outcome after stroke. ICAM-1 $-/-$ mice ($n = 13$) were significantly protected from the effects of focal cerebral ischemia and reperfusion, based on a 3.7-fold reduction in infarct volume ($P < 0.01$) compared with ICAM-1 $+/+$ controls (Figs. 6 and 7 A). This reduction in infarct volume was accompanied by reduced neurologic deficit (Fig. 7 B) and increased postreperfusion cerebral cortical blood flow (Fig. 7 C). Given these results, it was not surprising that mortality was also significantly decreased in the ICAM-1 $-/-$ mice compared with ICAM-1 $+/+$ controls (15 vs. 50%, $P < 0.05$; Fig. 7 D).

Discussion

Epidemiologic evidence in humans suggests that neutrophils contribute to the initiation of stroke (38) as well as to cerebral



Figure 4. Expression of ICAM-1 antigen in the cerebral microvasculature 24 h after middle cerebral artery occlusion. A coronal section of brain was obtained for ICAM-1 immunostaining, so that the noninfarcted and infarcted hemispheres from the same brain could be compared under identical staining conditions. Staining was performed using a rat anti-murine ICAM-1 antibody, with sites of primary antibody binding visualized by alkaline phosphatase. (A) Cerebral microvessel in the contralateral (noninfarcted) section of a brain obtained 24 h after middle cerebral artery occlusion. (B) Cerebral microvessel from the ipsilateral (infarcted) hemisphere from the same section of brain as shown in A. Endothelial cells from ipsilateral cerebral microvessels demonstrate increased expression of ICAM-1 (bright red staining). $\times 250$.

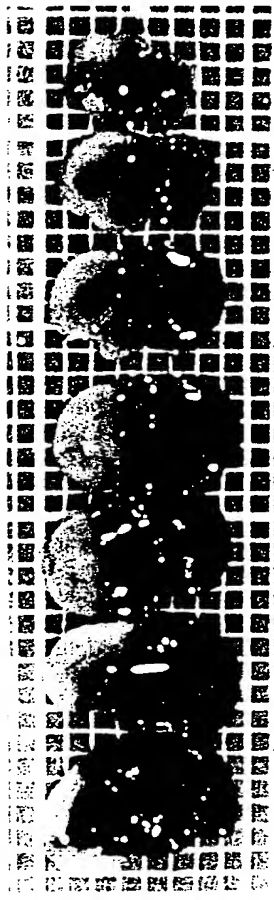


Wild Type



ICAM-1 (-/-)

Figure 5. Cerebrovascular anatomy in homozygous null ICAM-1 mice (right) and wild-type controls (left). India ink staining of cerebrovascular anatomy with an inferior view of the circle of Willis demonstrates that there were no gross anatomic differences in the vascular pattern of the cerebral circulation, with intact posterior communicating arteries in both.



Wild Type



ICAM-1 (-/-)

Figure 6. TTC-stained serial sections at 24 h from representative wild-type (left) or homozygous null ICAM-1 mice (right) subjected to transient middle cerebral artery occlusion. The pale white area in the middle cerebral artery territory represents infarcted brain tissue.

tissue injury and poor clinical outcome (39), with a potential role for neutrophils in postischemic hypoperfusion, neuronal dysfunction, and scar formation (40–44). Although there is considerable experimental evidence which suggests that neutrophils can exacerbate tissue damage after stroke (13, 45–48), certain pieces of experimental data have stoked controversy by failing to find an association between agents which block neutrophil accumulation and indices of stroke outcome. In a rat model of stroke, antibody-mediated depletion of neutrophils before stroke significantly decreased brain water content and infarct size (13). However, cyclophosphamide-induced leukocytopenia in a gerbil model (49) or antineutrophil antibody administration to dogs (50) showed no beneficial effects in global models of cerebral ischemia. Experimental therapy targeted at interfering with neutrophil–endothelial interactions has also produced mixed results. In a feline model of transient focal cerebral ischemia, treatment with antibody to CD18 (the common subunit of β_2 integrins, which bind to intercellular adhesion molecule-1 [reference 51]) did not alter recovery of cerebral blood flow, return of evoked potentials, or infarct volume (23). However, other experiments have found that microvascular patency after transient focal ischemia in primates is improved by antibodies to CD18 (14). In a similar rat model, anti-CD11b/CD18 antibody has also been shown to reduce both neutrophil accumulation and ischemia-related neuronal damage (52).

The experiments reported here show that, in a murine model of focal cerebral ischemia and reperfusion, neutrophils accumulate in postischemic cerebral tissue, a finding corroborated in other models which similarly demonstrate increased granulocyte accumulation in areas of low cerebral blood flow early during the postischemic period (15, 16, 36, 45). Not only do neutrophils accumulate during the postischemic period in mice, but their presence exacerbates indices of stroke outcome. When animals were made neutropenic before the is-

whereas viable tissue stains brick red. Quantification of infarct volumes by planimetry of serial cerebral sections in multiple experiments is shown in Fig. 7A.

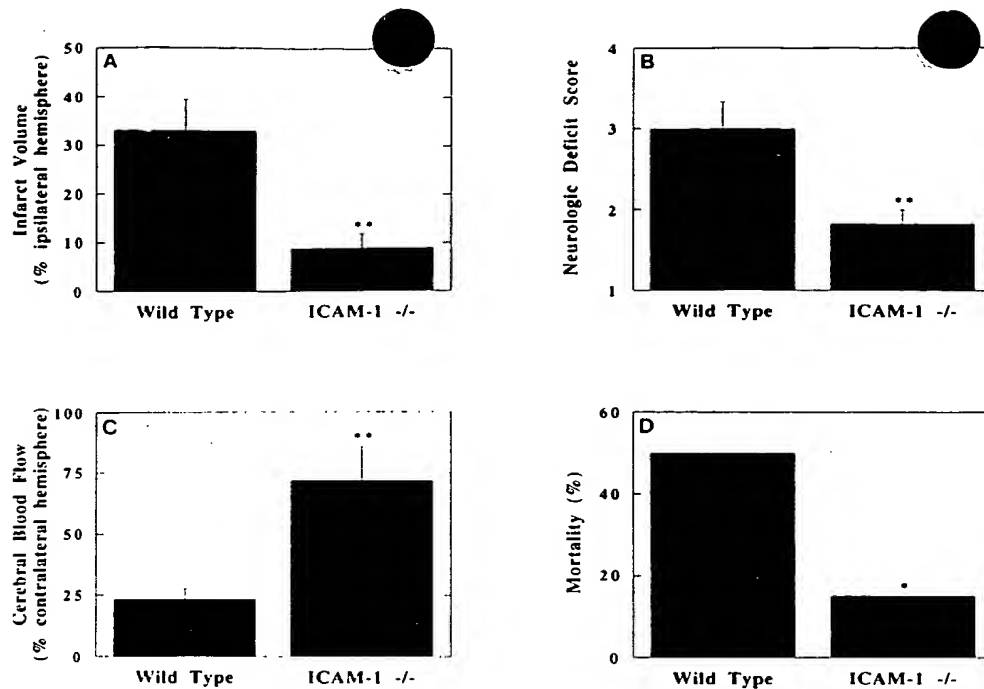


Figure 7. Role of ICAM-1 in stroke outcome. Transient middle cerebral artery occlusion was performed as described in ICAM-1 +/+ (Wild Type, $n = 16$) or ICAM-1 -/- ($n = 13$) mice, and indices of stroke outcome were measured as described in Fig. 2. (A) Effect of ICAM-1 on infarct volume, (B) neurologic deficit score, (C) cerebral blood flow, and (D) mortality. * $P < 0.05$, ** $P < 0.01$.

chemic event, cerebral infarcts were smaller, with improved cerebral perfusion after the ischemic event. These data are quite similar to those reported in a rabbit model of thromboembolic stroke, in which immunodepletion of neutrophils resulted both in reduced infarction volume and improved blood flow (35). Because neutrophils contribute to murine postischemic cerebral injury, we were able to pursue a strategy to elucidate the role of ICAM-1 in the pathophysiology of stroke using deletionally mutant ICAM-1 mice (24). Our experiments indicate that homozygous null ICAM-1 mice are relatively resistant to the deleterious effects of cerebral ischemia and reperfusion.

To demonstrate the role of both neutrophils and ICAM-1 in the pathogenesis of tissue injury in stroke, the studies reported here used several methods for assessing stroke outcome. Although numerous investigators have used TTC staining to quantify cerebral infarct volumes (26, 30–32, 37, 53), there has been some controversy as to the accuracy of this method, especially when evaluated early after the ischemic event. In the TTC method, TTC reacts with intact oxidative enzymes on mitochondrial cristae and is thereby reduced to a colored formazan (54). TTC staining is unreliable before 2 h of ischemia have elapsed; beyond 36 h, cells infiltrating into the infarcted tissue can stain positively with TTC, thereby obscuring the clear demarcation between infarcted and noninfarcted tissues seen with earlier staining (31). Although the size of the infarct delineated by TTC staining correlates well with infarct size delineated by hematoxylin and eosin staining (30, 32), direct morphometric measurements tend to overestimate infarct volumes due to cerebral edema, especially during the first 3 d after the ischemic event (32). Even given these limitations, however, the studies reported here incorporate three additional methods to define the role of neutrophils and ICAM-1 in stroke outcome, including neurologic deficit score, relative cerebral blood flow to the affected area, and mortality. These additional measures, which do not depend upon the accuracy

of TTC staining, contribute strongly to our identification of a pathogenic role for both neutrophils and ICAM-1 in stroke.

There has been a recent profusion of scientific studies exploring the mechanistic basis for neutrophil recruitment to postischemic tissues. Endothelial cells appear to be the chief regulators of neutrophil traffic, regulating the processes of neutrophil chemoattraction, adhesion, and emigration from the vasculature (55). When exposed to a hypoxic environment as a paradigm for tissue ischemia, endothelial cells synthesize the potent neutrophil chemoattractant and activator IL-8 (9), the blockade of which appears to be beneficial in a lung model of ischemia and reperfusion (6). In addition, hypoxic endothelial cells synthesize the proinflammatory cytokine IL-1 (8), which can upregulate endothelial expression of the neutrophil adhesion molecules E-selectin and ICAM-1 in an autocrine fashion (8, 9, 56). Other neutrophil adhesion mechanisms may also be activated in the brain after ischemia, such as release of P-selectin from preformed storage pools within Weibel-Palade body membranes (10). In a primate model, P-selectin expression was rapidly and persistently enhanced after focal middle cerebral artery ischemia and reperfusion (18). Although P-selectin-dependent neutrophil recruitment appears to be deleterious after cardiac ischemia and reperfusion (57), its pathophysiologic relevance in the setting of stroke has not yet been determined. While hypoxia induces de novo synthesis of the bioactive lipid PAF (11), in a spinal cord ischemia reperfusion model, PAF antagonism offered no incremental benefit when given simultaneously with antibody to CD11/CD18 (48).

Understanding the role of ICAM-1 in the pathophysiology of stroke appears to be of particular relevance in humans for several reasons. Increased cerebrovascular ICAM-1 expression has been demonstrated in primates by 4 h of ischemia and reperfusion, particularly in the lenticulostriate microvasculature (18). An autopsy study of recent cerebral infarcts in humans also demonstrated increased ICAM-1 expression (20). Since rats also express cerebral vascular ICAM-1 within 24 h

in both a photochemically induced model of rat cerebral ischemia (19) and a middle cerebral artery occlusion model (12), these data suggested the potential usefulness of transgenic ICAM-1-deficient mice in elucidating the pathophysiologic significance of increased postcerebral ischemic ICAM-1 expression. In particular, the time frame of ICAM-1 expression (increased by 4–24 h) in these models suggests that ICAM-1-mediated neutrophil-endothelial interactions may be targeted in future pharmacologic strategies to improve human stroke outcome, as this time frame represents a realistic clinical window for therapeutic intervention.

Although neutropenic animals demonstrated increased regional cerebral blood flow compared with controls, compared with neutropenic animals, ICAM-1-deficient mice tended to have even higher ipsilateral cerebral blood flows at 24 h. This observation may relate to the no-reflow phenomenon, wherein blood flow fails to return to preobstruction levels even after release of a temporary vascular occlusion. A significant body of previous work has implicated neutrophil plugging of capillary microvascular beds in this process (58), although in a model of global cerebral ischemia, an 85% reduction in the circulating leukocyte count did not decrease the incidence or severity of reflow failure (49). Our data suggest that non-neutrophil-dependent mechanisms, which nevertheless involve ICAM-1, may contribute to cerebrovascular postischemic no-reflow. Since macrophages and lymphocytes both express LFA-1, which mediates an adhesive interaction with endothelial cell ICAM-1 (51), it is possible that ICAM-1-deficient mice have diminished recruitment of these mononuclear cells, a possibility which is currently the subject of further investigation in our laboratory. This hypothesis is supported by multiple pathologic observations demonstrating macrophage and lymphocyte accumulation by 1–3 d after cerebral infarction (12, 17, 19, 34, 59).

Taken together, our studies indicate that, in a murine model of focal cerebral ischemia and reperfusion, neutrophils accumulate in the infarcted hemisphere and that neutropenic animals demonstrate cerebral protection. Increased expression of ICAM-1 on cerebral endothelial cells appears to be an important mechanism driving this neutrophil recruitment, and mice which are unable to express ICAM-1 demonstrate improved postischemic blood flows, reduced infarction volumes, and reduced mortality. These data suggest that pharmacologic strategies targeted at interfering with neutrophil-endothelial interactions may improve the outcome after stroke in humans.

Acknowledgments

We thank Daniel Batista and Yu Shan Zou for their expert technical assistance with these studies.

This work was supported in part by a Grant-in-Aid from the American Heart Association and the Public Health Service (HD13063, HL42507, and HL50629). C. J. Winfree was the recipient of an American Heart Association Medical Student Scholarship in Cerebrovascular Disease and a Glorney-Raisbeck Medical Student Award, and D. J. Pinsky is a Clinician-Scientist of the American Heart Association.

References

1. Naka, Y., D. M. Stern, and D. J. Pinsky. 1995. Acute myocardial infarction: pathophysiology and biochemistry of ischemia, necrosis, and reperfusion. In *Atherosclerosis and Coronary Artery Disease*. V. Fuster, R. Ross, and E.

Topol, editors. Raven Press, New York, in press.

2. Pinsky, D., M. Oz, H. Liao, J. Morris, J. Brett, A. Morales, M. Karakurum, M. Van Lookeren Campagne, R. Nowogrod, and D. Stern. 1993. Restoration of the cyclic AMP second messenger pathway enhances cardiac preservation for transplantation in a heterotopic rat model. *J. Clin. Invest.* 92:2994–3002.
3. Pinsky, D. J., M. C. Oz, S. Koga, Z. Taha, M. J. Broekman, A. J. Marcus, H. Liao, Y. Naka, J. Brett, P. J. Cannon, et al. 1994. Cardiac preservation is enhanced in a heterotopic rat transplant model by supplementing the nitric oxide pathway. *J. Clin. Invest.* 93:2291–2297.
4. Lucchesia, B. R., S. W. Werns, and J. C. Fantone. 1989. The role of the neutrophil and free radicals in ischemic myocardial injury. *J. Mol. Cell. Cardiol.* 21:1241–1251.
5. Pinsky, D. J., Y. Naka, N. C. Chowdhury, H. Liao, M. C. Oz, R. E. Michler, E. Kubaszewski, T. Malinski, and D. M. Stern. 1994. The nitric oxide/cyclic GMP pathway in organ transplantation: critical role in successful lung preservation. *Proc. Natl. Acad. Sci. USA* 91:12086–12090.
6. Sekido, N., N. Mukaida, A. Harada, I. Nakanishi, Y. Watanabe, and K. Matsushima. 1993. Prevention of lung reperfusion injury in rabbits by a monoclonal antibody against interleukin-8. *Nature (Lond.)* 365:654–657.
7. Granger, D. 1988. Role of xanthine oxidase and granulocytes in ischemia-reperfusion injury. *Am. J. Physiol.* 255:H1269–H1275.
8. Shreenivas, R., S. Koga, M. Karakurum, D. Pinsky, E. Kaiser, J. Brett, B. A. Wolitzky, C. Norton, J. Plocinski, W. Benjamin, et al. 1992. Hypoxia-mediated induction of endothelial cell interleukin-1 α . An autocrine mechanism promoting expression of leukocyte adhesion molecules on the vessel surface. *J. Clin. Invest.* 90:2333–2339.
9. Karakurum, M., R. Shreenivas, J. Chen, D. Pinsky, S. D. Yan, M. Anderson, K. Sunouchi, J. Major, T. Hamilton, K. Kuwabara, et al. 1994. Hypoxic induction of interleukin-8 gene expression in human endothelial cells. *J. Clin. Invest.* 93:1564–1570.
10. Geng, J.-G., M. P. Bevilacqua, K. L. Moore, T. M. McIntyre, S. M. Prescott, J. M. Kim, G. A. Bliss, G. A. Zimmerman, and R. P. McEver. 1990. Rapid neutrophil adhesion to activated endothelium mediated by GMP-140. *Nature (Lond.)* 343:757–760.
11. Arnould, T., C. Michiels, and J. Remacle. 1993. Increased PMN adherence on ECs after hypoxia: involvement of PAF, CD11/CD18, and ICAM-1. *Am. J. Physiol.* 264:C1102–C1110.
12. Schroeter, M., S. Jander, O. W. Witte, and G. Stoll. 1994. Local immune responses in the rat cerebral cortex after middle cerebral artery occlusion. *J. Neuroimmunol.* 55:195–203.
13. Matsuo, Y., H. Onodera, Y. Shiga, M. Nakamura, M. Ninomiya, T. Kihara, and K. Kogure. 1994. Correlation between myeloperoxidase-quantified neutrophil accumulation and ischemic brain injury in the rat: effects of neutrophil depletion. *Stroke* 25:1469–1475.
14. Mori, E., G. J. del Zoppo, J. D. Chambers, B. R. Copeland, and K. E. Arfors. 1992. Inhibition of polymorphonuclear leukocyte adherence suppresses no-reflow after focal cerebral ischemia in baboons. *Stroke* 23:712–718.
15. Ohrenovitch, T. P., K. K. Kumaroo, and J. M. Hallenbeck. 1984. Autoradiographical detection of indium-111-labeled platelets in brain tissue section. *Stroke* 15:1049–1056.
16. Hallenbeck, J. M., A. J. Dutka, T. Tanishima, P. M. Kochanek, K. K. Kumaroo, C. B. Thompson, T. P. Ohrenovitch, and T. J. Contreras. 1986. Polymorphonuclear leukocyte accumulation in brain regions with low blood flow during the early postischemic period. *Stroke* 17:246–253.
17. Garcia, J. H., and Y. Kamijyo. 1974. Cerebral infarction: evolution of histopathological changes after occlusion of a middle cerebral artery in primates. *J. Neuropathol. & Exp. Neurol.* 33:408–421.
18. Okada, Y., B. R. Copeland, E. Mori, M. M. Tung, W. S. Thomas, and G. J. del Zoppo. 1994. P-selectin and intercellular adhesion molecule-1 expression after focal brain ischemia and reperfusion. *Stroke* 25:202–211.
19. Jander, S., M. Kraemer, M. Schroeter, O. W. Witte, and G. Stoll. 1995. Lymphocytic infiltration and expression of intercellular adhesion molecule-1 in photochemically induced ischemia in the rat cortex. *J. Cereb. Blood Flow Metab.* 15:42–51.
20. Sobel, R. A., M. E. Mitchell, and G. Fondren. 1990. Intercellular adhesion molecule-1 in cellular immune reactions in the human central nervous system. *Am. J. Pathol.* 136:337–354.
21. Clark, W. M., K. P. Madden, R. Rothlein, and J. A. Zivin. 1991. Reduction of central nervous system ischemic injury by monoclonal antibody to intercellular adhesion molecule. *J. Neurosurg.* 75:623–627.
22. Clark, W. M., K. P. Madden, R. Rothlein, and J. A. Zivin. 1991. Reduction of central nervous system ischemic injury in rabbits using leukocyte adhesion antibody treatment. *Stroke* 22:877–883.
23. Takeshima, R., J. R. Kirsch, R. C. Koehler, A. W. Gomoll, and R. J. Traystman. 1992. Monoclonal leukocyte antibody does not decrease the injury of transient focal cerebral ischemia in cats. *Stroke* 23:247–252.
24. Xu, H., J. A. Gonzalo, Y. St. Pierre, I. R. Williams, T. S. Kupper, R. S. Cotran, T. A. Springer, and J.-C. Gutierrez-Ramos. 1994. Leukocytosis and resistance to septic shock in intercellular adhesion molecule-1-deficient mice. *J. Exp. Med.* 180:95–109.
25. Hodes, R. J., B. S. Handwerger, and W. D. Terry. 1974. Synergy between subpopulations of mouse spleen cells in the in vitro generation of cell-

- mediated cytotoxicity: involvement of a cell. *J. Exp. Med.* 140:1646-1659.
26. Connolly, E. S., C. J. Winfree, D. M. Stern, R. A. Solomon, and D. J. Pinsky. 1996. Procedural and strain-related variables significantly affect outcome in a murine model of focal cerebral ischemia. *Neurosurgery (Baltimore)*. In press.
27. Dirnagl, U., B. Kaplan, M. Jacewicz, and W. Bulsinielli. 1989. Continuous measurement of cerebral blood flow by laser-doppler flowmetry in a rat stroke model. *J. Cereb. Blood Flow Metab.* 9:589-596.
28. Menzies, S. A., J. T. Hoff, and A. L. Betz. 1992. Middle cerebral artery occlusion in rats: a neurological and pathological evaluation of a reproducible model. *Neurosurgery (Baltimore)*. 31:100-107.
29. Bederson, J. B., L. H. Pitts, and M. Tsuji. 1986. Rat middle cerebral artery occlusion: evaluation of the model and development of a neurologic examination. *Stroke*. 17:472-476.
30. Bederson, J. B., L. H. Pitts, M. C. Nishimura, R. L. Davis, and H. M. Bartkowski. 1986. Evaluation of 2,3,5-triphenyltetrazolium chloride as a stain for detection and quantification of experimental cerebral infarction in rats. *Stroke*. 17:1304-1308.
31. Liszczak, T. C., E. T. Hedley-Whyte, J. F. Adams, D. H. Han, V. S. Koluri, F. X. Vacanti, R. C. Heros, and N. T. Zervas. 1984. Limitations of tetrazolium salts in delineating infarcted brain. *Acta Neuropathol.* 65:150-157.
32. Lin, T.-N., Y. Y. He, G. Wu, M. Khan, and C. Y. Hsu. 1993. Effect of brain edema on infarct volume in a focal cerebral ischemia model in rats. *Stroke*. 24:117-121.
33. Ballantyne, C. M., C. A. Kozak, W. E. O'Brien, and A. L. Beaudet. 1991. Assignment of the gene for intercellular adhesion molecule-1 (Icam-1) to proximal mouse chromosome 9. *Genomics*. 9:547-550.
34. Kochanek, P. M., and J. M. Hallenbeck. 1992. Polymorphonuclear leukocytes and monocytes/macrophages in the pathogenesis of cerebral ischemia and stroke. *Stroke*. 23:1367-1379.
35. Bednar, M. M., S. Raymond, T. McAuliffe, P. A. Lodge, and C. E. Gross. 1991. The role of neutrophils and platelets in a rabbit model of thromboembolic stroke. *Stroke*. 22:44-50.
36. Pozzilli, C., G. L. Lenzi, C. Argentino, A. Caroli, M. Rasura, A. Signore, L. Bozzao, and P. Pozzilli. 1985. Imaging of leukocytic infiltration in human cerebral infarcts. *Stroke*. 16:251-255.
37. Barone, F. C., D. J. Knudsen, A. H. Nelson, G. Z. Feuerstein, and R. N. Willette. 1993. Mouse strain differences in susceptibility to cerebral ischemia are related to cerebral vascular anatomy. *J. Cereb. Blood Flow Metab.* 13:683-692.
38. Prentice, R. L., T. P. Szatrowski, H. Kato, and M. W. Mason. 1982. Leukocyte counts and cerebrovascular disease. *J. Chronic Dis.* 35:703-714.
39. Pozilli, C., G. L. Lenzi, C. Argentino, L. Bozzao, M. Rasura, F. Giuabalei, and C. Fieschi. 1985. Peripheral white blood cell count in cerebral ischemic infarction. *Acta Neurol. Scand.* 71:396-400.
40. Ernst, E., A. Matrai, and F. Paulsen. 1987. Leukocyte rheology in recent stroke. *Stroke*. 18:59-62.
41. Groggaard, B., L. Schurer, B. Gerdin, and K. E. Arfors. 1989. Delayed hypoperfusion after incomplete forebrain ischemia in the rat: the role of polymorphonuclear leukocytes. *J. Cereb. Blood Flow Metab.* 9:500-505.
42. Hallenbeck, J. M., A. J. Dutka, P. M. Kochanek, A. Siren, G. H. Pezeshkpour, and G. Feuerstein. 1988. Stroke risk factors prepare rat brainstem tissues for modified local Schwartzman reaction. *Stroke*. 19:863-869.
43. Kintner, D. B., P. W. Kranner, and D. D. Gilboe. 1986. Cerebral vascular resistance following platelet and leukocyte removal from perfusate. *J. Cereb. Blood Flow Metab.* 6:52-58.
44. Mercuri, M., G. Ciuffetti, M. Robinson, and J. Toole. 1989. Blood cell rheology in acute cerebral infarction. *Stroke*. 20:959-962.
45. Clark, R. K., E. V. Lee, R. F. White, Z. L. Jonak, G. Z. Feuerstein, and F. C. Barone. 1994. Reperfusion following focal stroke hastens inflammation and resolution of ischemic injured tissue. *Brain Res. Bull.* 35:387-392.
46. Dutka, A. J., P. M. Kochanek, and J. M. Hallenbeck. 1989. Influence of granulocytopenia on canine cerebral ischemia induced by air embolism. *Stroke*. 20:390-395.
47. Clark, R. K., E. V. Lee, C. J. Fish, R. F. White, W. J. Price, Z. L. Jonak, G. Z. Feuerstein, and F. C. Barone. 1993. Development of tissue damage, inflammation and resolution following stroke: an immunohistochemical and quantitative planimetric study. *Brain Res. Bull.* 31:565-572.
48. Lindsberg, P. J., A. L. Siren, G. Z. Feuerstein, and J. M. Hallenbeck. 1995. Antagonism of neutrophil adherence in the deteriorating stroke model in rabbits. *J. Neurosurg.* 82:269-277.
49. Aspey, B. S., C. Jessimer, S. Pereira, and M. J. G. Harrison. 1989. Do leukocytes have a role in the cerebrovascular no-reflow phenomenon? *J. Neurol. Neurosurg. Psychiatry*. 52:526-528.
50. Schott, R. J., J. E. Natale, S. W. Ressler, R. E. Burney, and L. G. Alecy. 1989. Neutrophil depletion fails to improve outcome after cardiac arrest in dogs. *Ann. Emerg. Med.* 18:517-522.
51. Springer, T. A. 1990. Adhesion receptors of the immune system. *Nature (Lond.)*. 346:425-434.
52. Chopp, M., R. L. Zhang, H. Chen, Y. Li, N. Jiang, and J. R. Rusche. 1994. Postischemic administration of an anti-Mac-1 antibody reduces ischemic cell damage after transient middle cerebral artery occlusion in rats. *Stroke*. 25:869-876.
53. Huang, Z., P. L. Huang, N. Panahian, T. Dalkara, M. C. Fishman, and M. A. Moskowitz. 1994. Effects of cerebral ischemia in mice deficient in neuronal nitric oxide synthase. *Science (Wash. DC)*. 265:1883-1885.
54. Nachlas, M. M., K. C. Tson, E. D. Souza, C. S. Chang, and A. M. Seligman. 1963. Cytochemical demonstration of succinic dehydrogenase by the use of a new p-nitrophenyl substituted ditetrazole. *J. Histochem. Cytochem.* 5:420-436.
55. Pinsky, D. J., and D. M. Stern. 1994. Hypoxia-induced modulation of endothelial cell function. In *Reperfusion Injury and Clinical Capillary Leak Syndrome*. B. Zikria, M. C. Oz, and R. W. Carlson, editors. Futura Publishing, Mt. Kisco, NY, 31-55.
56. Pober, J. 1988. Warner-Lambert Parke Davis Award Lecture: cytokine-mediated activation of vascular endothelium. *Am. J. Pathol.* 133:426-433.
57. Weyrich, A. S., N.-L. Ma, D. J. Lefer, K. H. Albertine, and A. M. Lefer. 1993. In vivo neutralization of P-selectin protects feline heart and endothelium in myocardial ischemia and reperfusion injury. *J. Clin. Invest.* 91:2620-2629.
58. Jerome, S. N., M. Dore, J. C. Paulson, C. W. Smith, and R. J. Korthuis. 1994. P-selectin and ICAM-1-dependent adherence reactions: role in the genesis of postischemic no-reflow. *Am. J. Physiol.* 266:H1316-H1321.
59. Sornas, R., H. Ostlund, and R. Muller. 1972. Cerebrospinal fluid cytology after stroke. *Arch. Neurol.* 26:489-501.